

$\Lambda_b^0 \rightarrow \Lambda(1520)\mu^+\mu^-$ Angular distribution: Theory Predictions and Prospects at LHCb

Felicia Volle



Beautiful and Charming Baryon Workshop

10th September 2024

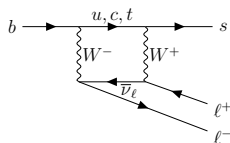
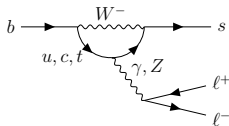
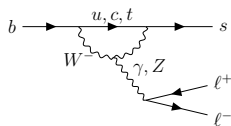


UNIVERSITY OF
BIRMINGHAM



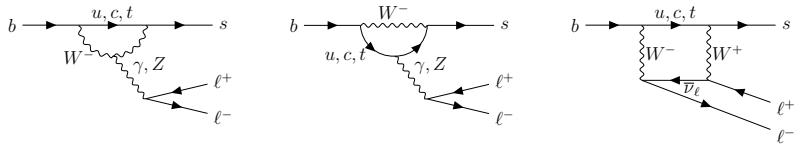
Why $b \rightarrow sl^+l^-$ decays are interesting to search for NP ?

$b \rightarrow sl^+l^-$ transitions are loop-mediated in the **Standard Model**.

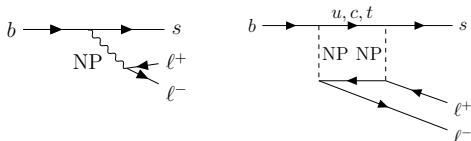


Why $b \rightarrow sl^+l^-$ decays are interesting to search for NP ?

$b \rightarrow sl^+l^-$ transitions are loop-mediated in the Standard Model.

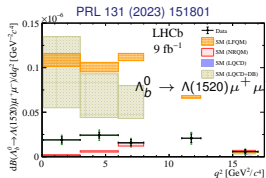
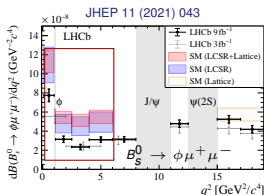
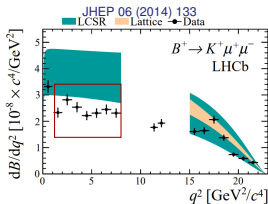


New Physics processes could contribute significantly.

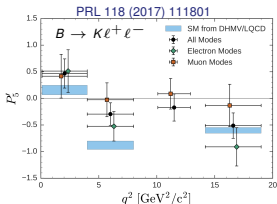
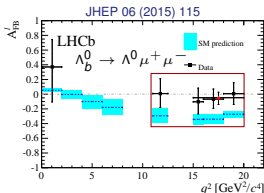
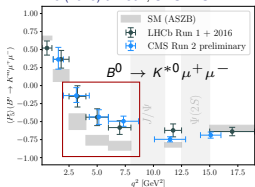


Experimental status

Promising channels to search for NP.



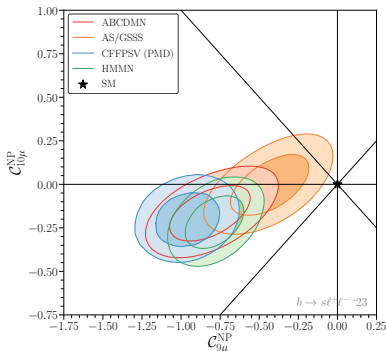
PRL 125 (2020) 011802, CMS-PAS-BPH-21-002



Deviations in differential branching fractions and angular observables.
LFU tests are mostly in agreement with SM hypothesis.

Global Effective Field Theory fits

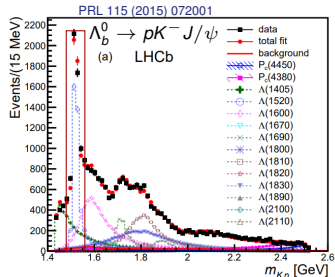
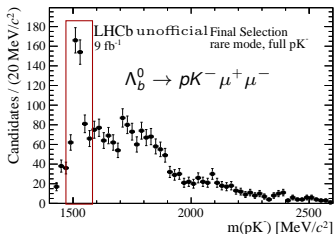
Global fits using different form factor predictions, different $b \rightarrow s\ell^+\ell^-$ observables, different assumptions about the non-local matrix elements and different statistical frameworks.



PoS (FPCP 2023) 010

Consistent deviations of $b \rightarrow s\mu^+\mu^-$ observables with respect to SM prediction.
Start exploration of new $b \rightarrow s\mu^+\mu^-$ decay channel in less explored b -baryon sector.

$\Lambda_b^0 \rightarrow pK^- \mu^+ \mu^-$ - my favorite decay



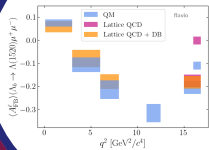
Why ?

- Most measurements performed with ***b*-meson decays**.
- *b*-baryons possess different **spin-structures**.
- $\Lambda(1520)$ narrow and abundant \Rightarrow few Λ^* contributions in $m(pK^-) \in [1.47, 1.57] \text{ GeV}/c^2$, which are studied later.
- **Theoretical** predictions are available for the differential branching fraction (BF) and form factors.

Focus on $\Lambda(1520)$.

MoM model-independent measurement including full $m(pK^-)$ spectrum is in progress.

Strategy



Angular
fit model

Λ_b^0 mass fit

Angular
acceptance

Angular
fit on data

LHCb detector

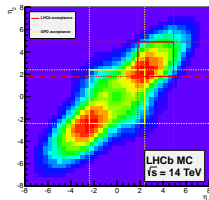
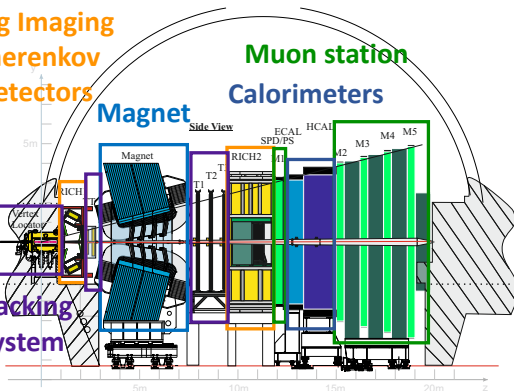
- $b\bar{b}$ production mostly in forward region
- Forward spectrometer with excellent tracking, momentum resolution, particle identification and a versatile and efficient trigger.

Ring Imaging
Cherenkov
detectors

Magnet

Muon station
Calorimeters

Tracking
system

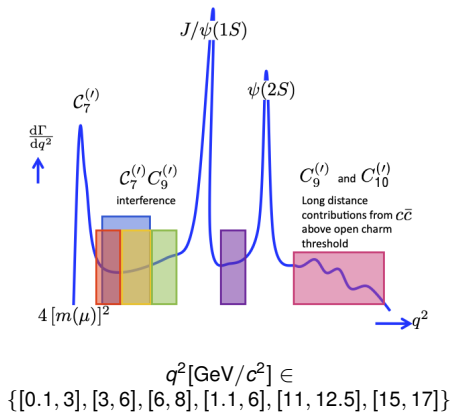


Some numbers

- * Good vertex and impact parameter resolution
 $\sigma_{IP} = 15 + 29/p_T$ mm.
- * Excellent momentum resolution $\approx 25 \text{ MeV}/c^2$ for two-body decays.
- * Excellent PID, e.g. μ ID 97% and $\pi \rightarrow \mu$ misID of 1-3%.
- * Versatile & efficient trigger system.

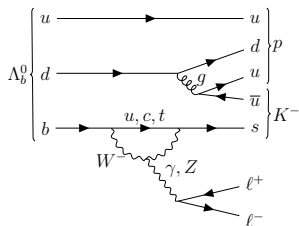
Analysis strategy

$$\mathcal{H}_{\text{eff}} = -\frac{4G_F}{\sqrt{2}} V_{tb} V_{ts}^* \sum_i (C_i \mathcal{O}_i + C'_i \mathcal{O}'_i)$$

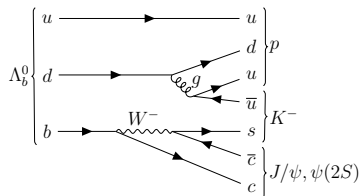


Exploit full Run 1 and 2 dataset of 9 fb^{-1} .

Rare mode:

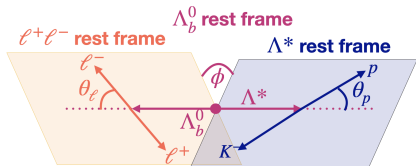


Resonant mode:



Differential branching fraction and angular observables

JHEP 06(2019)136



$(\theta_\ell, \theta_p, \phi)$ in helicity basis

Λ_b^0 assumed to be unpolarized.

$$d\vec{\Omega} = d \cos \theta_\ell d \cos \theta_p d\phi$$

$$\frac{d^4\Gamma}{dq^2 d\vec{\Omega}} = \sum_i \text{physics}_i \times \text{kinematics}_i$$

$$= \frac{3}{8\pi} \sum_i L_i(q^2, \mathcal{C}, ff) \times f_i(\vec{\Omega})$$

\mathcal{C} = Wilson Coefficients \rightarrow short distance part \rightarrow sensitive to NP
 ff = form factors \rightarrow long distance part

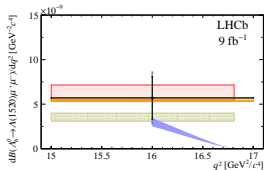
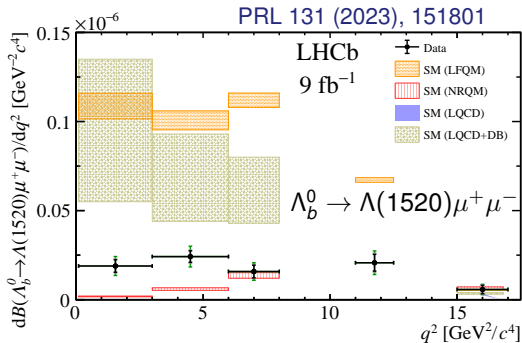
Observables :

$$S_i = \frac{L_i + \bar{L}_i}{d(\Gamma + \bar{\Gamma})/dq^2}, A_i = \frac{L_i - \bar{L}_i}{d(\Gamma + \bar{\Gamma})/dq^2},$$

$$A_{\text{FB}}^\ell = \frac{3(L_{1c} + 2L_{2c})}{2(L_{1cc} + 2(L_{1ss} + L_{2cc} + 2L_{2ss} + L_{3ss}))}$$

A_{FB}^ℓ is averaged over the Λ_b^0 and $\bar{\Lambda}_b^0$ decays.

Differential branching fraction measurement



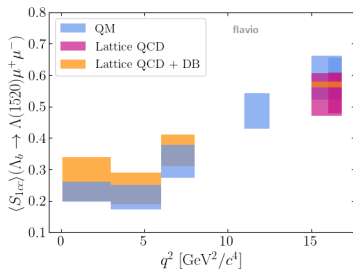
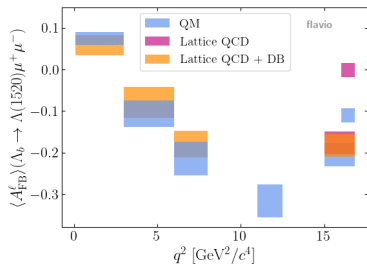
Good agreement in the high q^2 bin. More theoretical work is needed to understand the SM predictions in the low q^2 bins.

Theoretical prediction of angular observables

Binned angular observables using **non-relativistic Quark Model (QM)**, **Lattice QCD** and **joint Lattice QCD and dispersive bound (DB)** form factors.

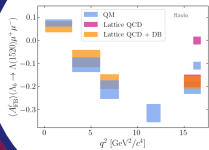
Lattice QCD prediction available in $q^2 \in [16, 16.81] \text{ GeV}^2/c^4$ bin.

JHEP 06 (2020) 102, Int.J.Mod.Phys.A 27 (2012) 1250016, PRD 103 (2021) 074505, JHEP 02 (2023) 010.

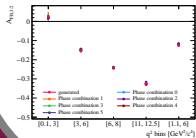


Angular observable values using Lattice QCD + DB and QM form factor predictions are in agreement with each other.

Strategy



Angular fit model



Λ_b^0 mass fit

Angular acceptance

Angular fit on data

Angular PDF of $\Lambda_b \rightarrow \Lambda(1520)\mu^+\mu^-$ decays

Simplifications :

- 1 Heavy quark limit ($m_b \rightarrow \infty$)
- 2 Normalization ($\frac{d\Gamma}{dq^2} = 1$):
 $1/2L_{1cc} + L_{1ss} = 1$
 $A_{FB,3/2}^{\ell} = 3/4L_{1c}$
- 3 CP-average ($L_i \rightarrow S_i$)

$$\begin{aligned} & \frac{8\pi}{3} \frac{d^4\Gamma}{dq^2 d \cos \theta_{\ell} d \cos \theta_{\Lambda^*} d\phi} \\ &= \cos^2 \theta_{\Lambda^*} (L_{1c} \cos \theta_{\ell} + L_{1cc} \cos^2 \theta_{\ell} + L_{1ss} \sin^2 \theta_{\ell}) \\ & \quad + \sin^2 \theta_{\Lambda^*} (L_{2c} \cos \theta_{\ell} + L_{2cc} \cos^2 \theta_{\ell} + L_{2ss} \sin^2 \theta_{\ell}) \\ & \quad + \sin^2 \theta_{\Lambda^*} (L_{3ss} \sin^2 \theta_{\ell} \cos^2 \phi + L_{4ss} \sin^2 \theta_{\ell} \sin \phi \cos \phi) \\ & \quad + \sin \theta_{\Lambda^*} \cos \theta_{\Lambda^*} \cos \phi (L_{5s} \sin \theta_{\ell} + L_{5sc} \sin \theta_{\ell} \cos \theta_{\ell}) \\ & \quad + \sin \theta_{\Lambda^*} \cos \theta_{\Lambda^*} \sin \phi (L_{6s} \sin \theta_{\ell} + L_{6sc} \sin \theta_{\ell} \cos \theta_{\ell}), \end{aligned}$$

JHEP 06 (2019) 136, Eur. Phys. J. Plus 136 (2021) 614

$$\begin{aligned} \text{PDF}_{\text{ang},3/2} &= \left(\left(1 - \frac{1}{2} S_{1cc} \right) (1 - \cos^2 \theta_{\ell}) + S_{1cc} \cos^2 \theta_{\ell} + \frac{4}{3} A_{FB,3/2}^{\ell} \cos \theta_{\ell} \right) \\ & \quad \times \left(\frac{1}{4} + \frac{3}{4} \cos^2 \theta_p \right) \end{aligned}$$

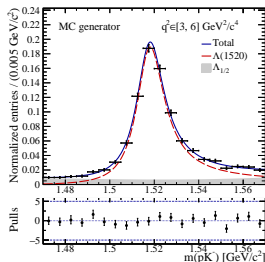
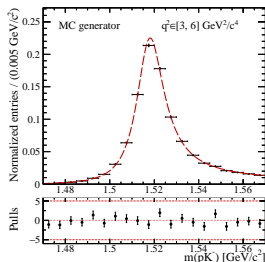
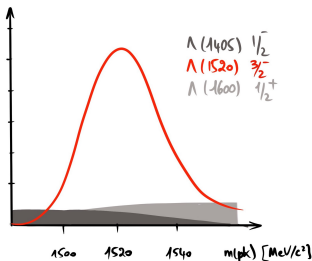
Angular PDF is only dependent on $\cos \theta_{\ell}$ and $\cos \theta_p$.

But there is not only the $\Lambda(1520)$!

Problem: Presence of $\Lambda(1520)$ and spin-1/2 Λ^* resonances in $m(pK^-)$ window.

Idea: Separation by $m(pK^-)$ fit.

- Need of relativistic Breit-Wigner to describe $\Lambda(1520)$ line shape.
- $\Lambda(1405)$ and $\Lambda(1600)$ described together by polynomial.



Angular shape of $\Lambda_b^0 \rightarrow \Lambda_{1/2} \mu^+ \mu^-$ (i.e. $\Lambda(1405)$, $\Lambda(1600)$)

Simplifications :

- 1 Strong decay :

$$\alpha = 0$$

- 2 Normalization:

$$K_{1cc} + 2K_{1ss} = 1$$

$$A_{\text{FB},1/2}^{\ell} = 3/2 K_{1c}$$

- 3 CP-average

$$K(q^2, \cos \theta_{\ell}, \cos \theta_{\Lambda}, \phi) \equiv \frac{8\pi}{3} \frac{d^4\Gamma}{dq^2 d\cos \theta_{\ell} d\cos \theta_{\Lambda} d\phi},$$

which can be decomposed in terms of a set of trigonometric functions,

$$\begin{aligned} K(q^2, \cos \theta_{\ell}, \cos \theta_{\Lambda}, \phi) = & (K_{1ss} \sin^2 \theta_{\ell} + K_{1cc} \cos^2 \theta_{\ell} + K_{1c} \cos \theta_{\ell}) \\ & + (K_{2ss} \sin^2 \theta_{\ell} + K_{2cc} \cos^2 \theta_{\ell} + K_{2c} \cos \theta_{\ell}) \cos \theta_{\Lambda} \\ & + (K_{3sc} \sin \theta_{\ell} \cos \theta_{\ell} + K_{3s} \sin \theta_{\ell}) \sin \theta_{\Lambda} \sin \phi \\ & + (K_{4sc} \sin \theta_{\ell} \cos \theta_{\ell} + K_{4s} \sin \theta_{\ell}) \sin \theta_{\Lambda} \cos \phi. \end{aligned}$$

JHEP 01 (2015) 155

$$\text{PDF}_{\text{ang},1/2} = \frac{1}{2} (1 - K_{1cc}) (1 - \cos^2 \theta_{\ell}) + K_{1cc} \cos^2 \theta_{\ell} + \frac{2}{3} A_{\text{FB},1/2}^{\ell} \cos \theta_{\ell}$$

Angular PDF is only dependent on $\cos \theta_{\ell}$.

K parameters encode information about $\Lambda_{1/2}$ resonances in $m_{\rho K}$ window.

Interferences between the Λ^* resonances negligible ?

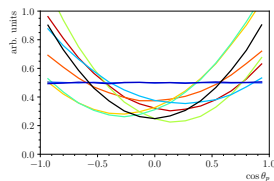
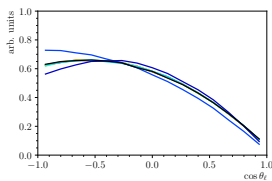
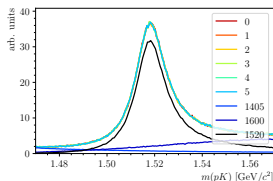
Strength of interferences **not predicted** by theory.

→ MC generator **generates** angular distribution of $\Lambda_b^0 \rightarrow \Lambda^* \mu^+ \mu^-$ with interfering $\Lambda(1405)$, $\Lambda(1520)$ and $\Lambda(1600)$ resonances.

→ **Random phase combinations** $e^{\pm i(\varphi_{1520} - \varphi_X)}$ generated to test different interference hypotheses.

JHEP 02 (2023) 189

phase combi	$\Delta\varphi_{1405}$	$\Delta\varphi_{1600}$
0	0.00π	0.00π
1	1.38π	1.93π
2	1.10π	1.61π
3	0.43π	0.62π
4	0.06π	1.38π
5	1.41π	0.70π



No impact of interferences on $m(pK^-)$ since different quantum numbers.

Negligible impact on $\cos \theta_\ell$.

Strong effect on $\cos \theta_\rho$ even with small $\Lambda_{1/2}$ amplitudes !

Angular fit model including interferences

Angular PDF of $\Lambda(1520)$ in HQ limit,
Summed angular PDF of the $\Lambda_{J=1/2}^*$ resonances,
Interferences between the three Λ^* resonances.

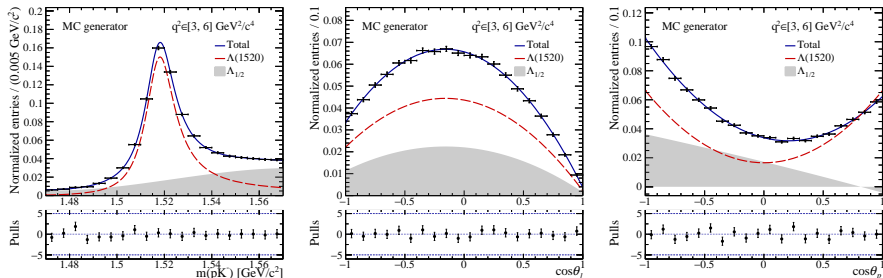
$$\begin{aligned} \text{PDF}_{\text{ang}}^{\text{Int},1/2} &= f_{3/2} \left(\left(1 - \frac{1}{2} S_{1\text{cc}} \right) \left(1 - \cos^2 \theta_\ell \right) + S_{1\text{cc}} \cos^2 \theta_\ell + \frac{4}{3} A_{\text{FB},3/2}^\ell \cos \theta_\ell \right) \\ &\quad \times \left(\frac{1}{4} + \frac{3}{4} \cos^2 \theta_p \right) \\ &+ (1 - f_{3/2}) \left(\frac{1}{2} (1 - K_{1\text{cc}}) \left(1 - \cos^2 \theta_\ell \right) + K_{1\text{cc}} \cos^2 \theta_\ell + \frac{2}{3} A_{\text{FB},1/2}^\ell \cos \theta_\ell \right) \\ &\quad \times \left(\frac{3 - i_2}{3} + i_1 \cos \theta_p + i_2 \cos^2 \theta_p \right) \end{aligned}$$

The observables of interest are $A_{\text{FB},3/2}^\ell$ and $S_{1\text{cc}}$.

Fit of dedicated MC samples

Fit MC samples with $\Delta\varphi_{1405} = \Delta\varphi_{1520} = 0$ hypothesis.

Projection of the $\Lambda(1520)$, $\Lambda_{1/2}$'s (including interference), total PDF.

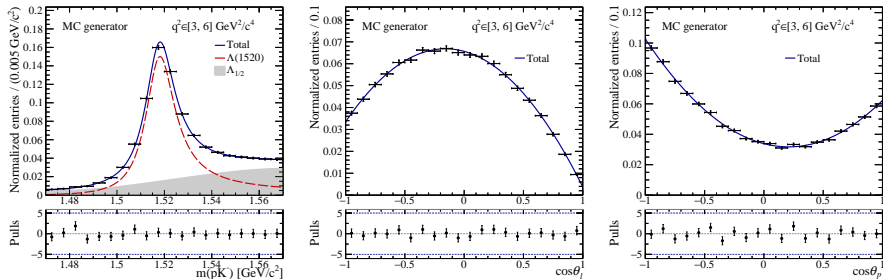


Interference terms cause $\text{PDF}_{\text{ang}}^{\text{Int},1/2}$ to be negative in some corners of the phase-space.

Fit of dedicated MC samples without constraining interference terms

Idea: Write $\text{PDF}_{\text{ang}}^{\text{Int}1/2}$ as one entire PDF to prevent from becoming negative.

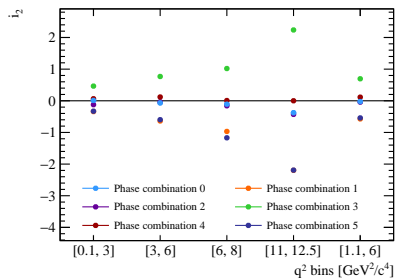
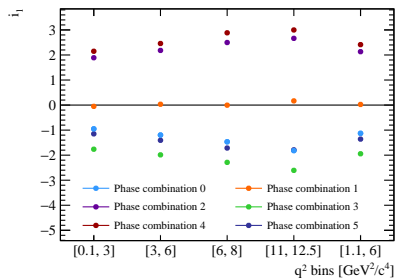
But: Cannot separate easily into $\text{PDF}_{\text{ang},1/2}$ and $\text{PDF}_{\text{ang},3/2}$.



Neither $f_{3/2}$, nor $1 - f_{3/2}$ constrain interference terms.

How do the interferences change between the samples ?

Interference term values from the fit of the dedicated MC samples.

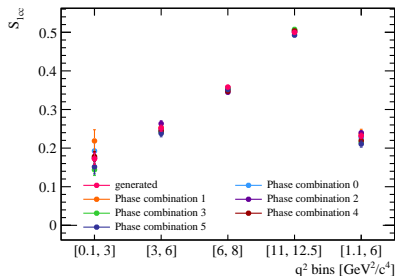
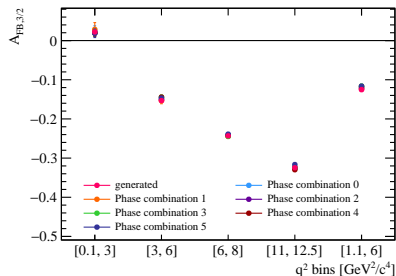


The interference terms differ between all the MC samples.

The fit model is able to account for all the phase combinations.

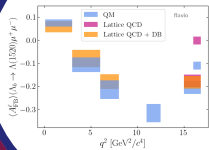
Stability of the angular observable fit values

Uncertainties are linked to sample size \rightarrow not scaled to data expectations.

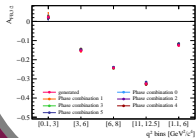


Although the different interference values, the fit is able to find the generated values of $A_{FB,3/2}^\ell$ and S_{1cc} .

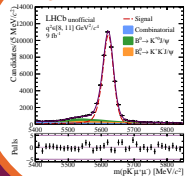
Strategy



Angular fit model



Λ_b^0 mass fit

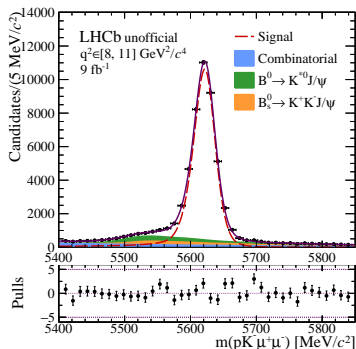


Angular acceptance

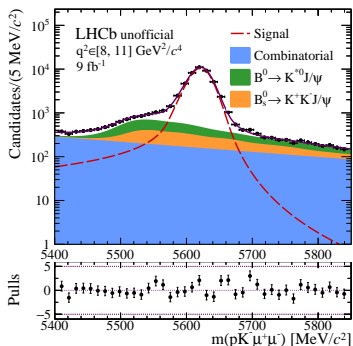
Angular fit on data

Λ_b^0 mass fit in the J/ψ bin to data

J/ψ unconstrained Λ_b^0 mass fit to the full Run 1 and 2 dataset.



(a) Linear scale

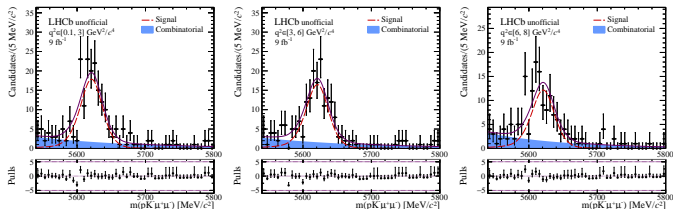


(b) Logarithmic scale

Λ_b^0 mass fit permits to subtract the background statistically.

Λ_b^0 mass fit in the rare mode

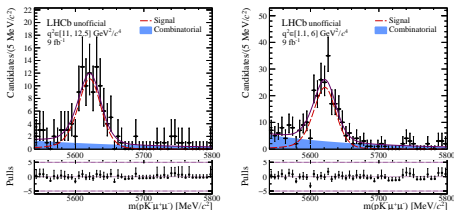
Combinatorial background and signal only.



(a) $q^2 \in [0.1, 3] \text{ GeV}^2/c^4$

(b) $q^2 \in [3, 6] \text{ GeV}^2/c^4$

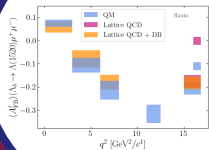
(c) $q^2 \in [6, 8] \text{ GeV}^2/c^4$



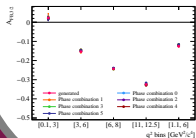
(d) $q^2 \in [11, 12.5] \text{ GeV}^2/c^4$

(e) $q^2 \in [1.1, 6] \text{ GeV}^2/c^4$

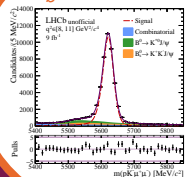
Strategy



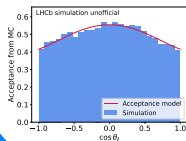
Angular fit model



Λ_b^0 mass fit



Angular acceptance



Angular fit on data

Angular acceptance model

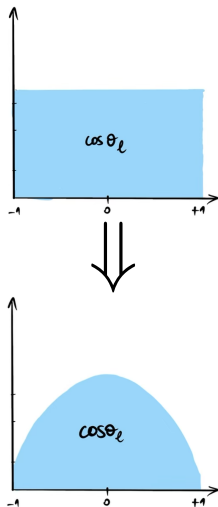
Why? Selection and corrections disturb angular distribution, which need to be accounted for.

- (1) Generation of phase-space simulation samples, which are flat in the angles.
- (2) Apply full selection and corrections.
- (3) Model unfactorized angular acceptance with Legendre P_ℓ and Fourier Polynomials P_f as

$$\varepsilon(\cos \theta_\ell, \cos \theta_p, \phi) = \sum_{ijk} c_{ijk} P_{\ell,i}(\cos \theta_\ell) P_{\ell,j}(\cos \theta_p) P_{f,k}(\phi).$$

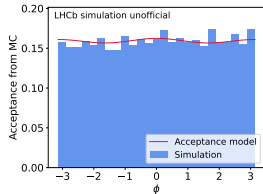
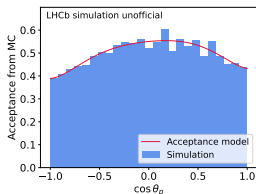
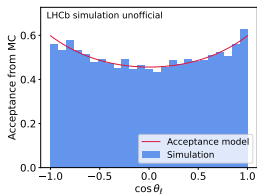
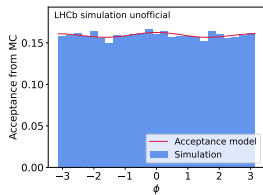
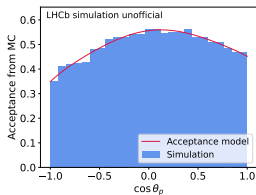
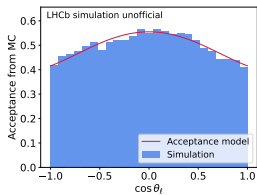
- (4) Calculate angular acceptance weights via Method of Moments.

$\cos \theta_\ell$ and ϕ modeled with even orders up to 4,
 $\cos \theta_p$ with all orders up to 6.



Extraction of angular acceptance

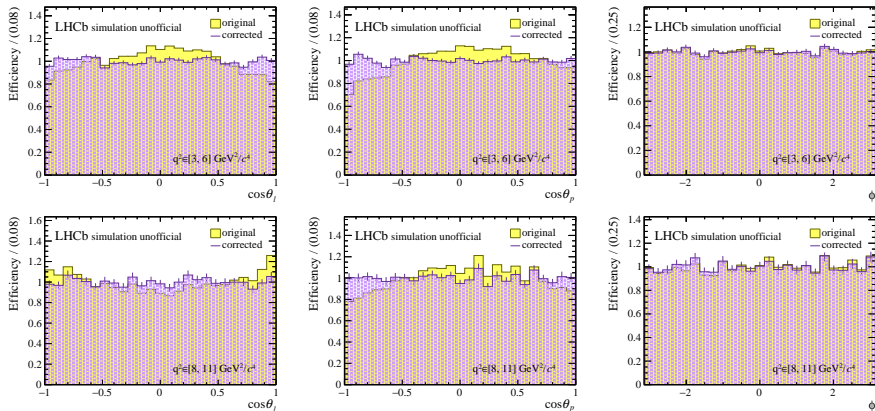
Exemple of $q^2 \in [3, 6] \text{ GeV}^2/c^4$ bin (top) and $[8, 11] \text{ GeV}^2/c^4$ (bottom)



Cross-check of angular acceptance event weights

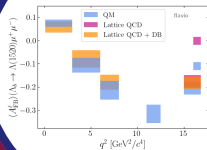
(1 solid) Angular shape of simulation sample after selection and corrections.

(2 line) Applying the inverse of the angular acceptance weights to same simulation sample should lead flat distributions.

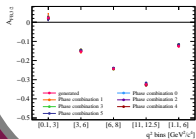


Method of moments checked to work ✓

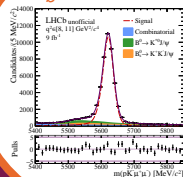
Strategy



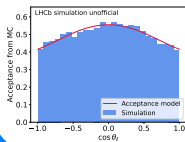
Angular fit model



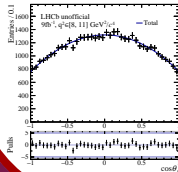
Λ_b^0 mass fit



Angular acceptance

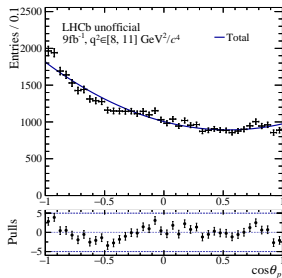
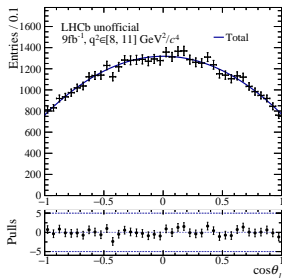
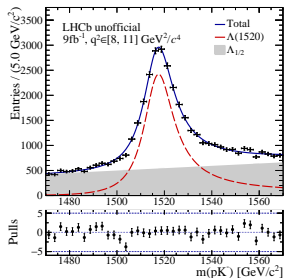


Angular fit on data



Angular fit of J/ψ control mode

Fits to background subtracted and acceptance corrected data with $sWeights$ from J/ψ unconstrained Λ_b^0 mass fit.

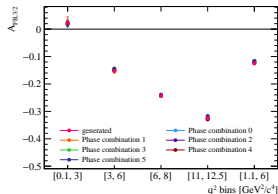
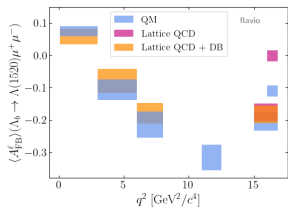


A_{FB}^{ℓ} compatible with zero within two standard deviations. ✓

Similar for the J/ψ constrained case.

Conclusion and outlook

- Studies of $b \rightarrow s \ell^+ \ell^-$ decays receiving attention since 15 years.
- First angular analysis in $\Lambda_b^0 \rightarrow \Lambda(1520) \mu^+ \mu^-$ decays is developed.
- Challenge of the analysis is the small sample size.
- Analysis with Run 1 and 2 data is statistically dominated. \Rightarrow More data is needed to fully exploit its potential.





Thank you for you
attention!

Bibliography

- [1] Bernard Breton, *Emperor penguin*, Encyclopædia Britannica, <https://www.britannica.com/animal/emperor-penguin> Accessed: 31/07/2023.
- [2] C. Burgard and D. Galbraith, *Example: Standard model of physics*, <https://texample.net/tikz/examples/model-physics/> 2016. Accessed: 01/04/2023.
- [3] Johan Jarnestad/The Royal Swedish Academy of Sciences, *The Nobel prize in Physics 2015: The chameleons of space*, <https://www.nobelprize.org/uploads/2018/06/popular-physicsprize2015.pdf> 2015. Accessed: 31/07/2023.
- [4] Ulrika Royen/The Royal Swedish Academy of Sciences, *The Nobel prize in Physics 2008: Unravelling the hidden symmetries of nature*, <https://www.nobelprize.org/prizes/physics/2008/popular-information/> 2008. Accessed: 31/07/2023.
- [5] NASA and WMAP Science Team, *Universe content - WMAP 9yr Pie Chart*, <https://map.gsfc.nasa.gov/media/121236/index.html> 2013. Accessed: 31/07/2023.

Λ_b^0 production polarisation

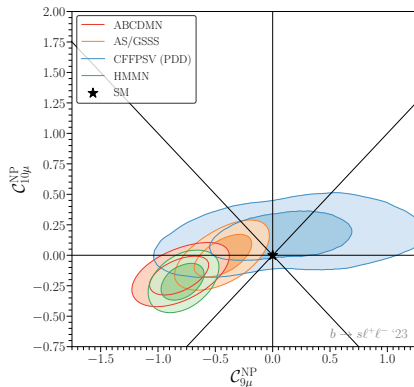
PL B 724 (2013) 27

- Substantial Λ_b^0 polarization measured by production in $e^-e^+ \rightarrow Z^0 \rightarrow b\bar{b}$.
- If Λ_b^0 polarization non-zero, $\Lambda_b^0 \rightarrow \Lambda^{(*)}\gamma$ decays probe photon polarisation.
- Assumption of equal polarisation between Λ_b^0 and $\bar{\Lambda}_b^0$.
- Analysis of $\Lambda_b^0 \rightarrow J/\psi\Lambda(\rightarrow p\pi^-)$ decays, produced in pp collisions.
- Analysing 1 fb^{-1} in pp collisions at 7 TeV.
- Λ_b^0 transverse production polarisation of $0.06 \pm 0.07(\text{stat}) \pm 0.02(\text{syst})$.

Λ_b^0 production polarisation measured to be in agreement with zero.

Global Effective Field Theory fits

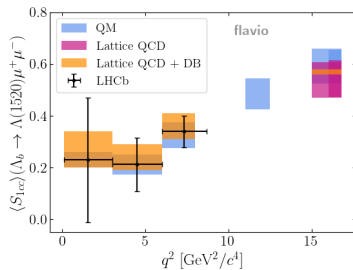
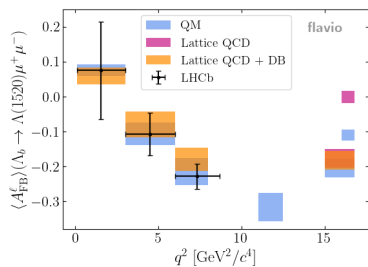
Global fits using different form factor predictions, different $b \rightarrow s\ell^+\ell^-$ observables, different assumptions about the non-local matrix elements and different statistical frameworks.



PoS (FPCP 2023) 010

Agreement with SM in data-driven treatment of hadronic uncertainties.

LHCb sensitivity



“Ideal case scenario”: Sensitivity for $\Lambda(1520)$ PDF only and without background.

Hypatia 2

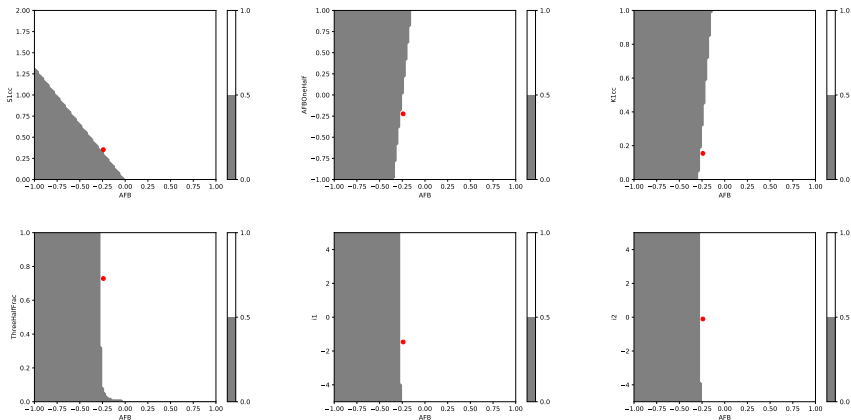
NIM A, 764, 150 (2014)

$$\text{Hypatia2}(x, \mu, \sigma, \lambda, \zeta, \beta, a_l, n_l, a_r, n_r) = \begin{cases} \frac{G(\mu - a_l, \sigma, \mu, \sigma, \lambda, \zeta, \beta)}{\left(1 - \frac{x}{n_l G(\dots) / G'(\dots) - a_l \sigma}\right)^{n_l}} & \text{if } \frac{x - \mu}{\sigma} < -a_l \\ \left((x - \mu)^2 + A_\lambda^2(\zeta) \sigma^2 \right)^{\frac{1}{2} \lambda - \frac{1}{4}} e^{\beta(x - \mu)} K_{\lambda - \frac{1}{2}} \left(\zeta \sqrt{1 + \left(\frac{x - \mu}{A_\lambda(\zeta) \sigma} \right)^2} \right) \equiv G(x, \mu, \dots) & \text{otherwise} \\ \frac{G(\mu + a_r, \sigma, \mu, \sigma, \lambda, \zeta, \beta)}{\left(1 - \frac{x}{n_r G(\dots) / G'(\dots) - a_r \sigma}\right)^{n_r}} & \text{if } \frac{x - \mu}{\sigma} > a_r \end{cases}$$

Hyperbolic core of a crystall-ball like function G and two tails.

Two-dimensional scan of the angular PDF

Angular observable values are the SM values from FLAVIO, here for the $q^2 \in [6, 8] \text{ GeV}^2/c^4$ bin.



Angular observable SM values are close to the physical boundary of the PDF.

Relativistic Breit-Wigner line shape

$$\begin{aligned}
 |\text{BW}_{\text{rel}}(m_{pK})|^2 &= q(m_{pK})\rho(m_{pK}) \left[\left(\frac{q(m_{pK})}{q(M_{\Lambda^*})} \right)^{L_{\Lambda_b \rightarrow \Lambda^* \mu\mu}} \left(\frac{p(m_{pK})}{p(M_{\Lambda^*})} \right)^{L_{\Lambda^* \rightarrow pK}} \right. \\
 &\quad \left. \times F_{\Lambda_b \rightarrow \Lambda^* \mu\mu}(q(m_{pK}), q(M_{\Lambda^*}), r_{\Lambda_b}) \frac{F_{\Lambda^* \rightarrow pK}(p(m_{pK}), p(M_{\Lambda^*}), r_{\Lambda^*})}{M_{\Lambda^*}^2 - m_{pK}^2 - iM_{\Lambda^*}\Gamma(m_{pK})} \right]^2 \\
 \Gamma(M_{pK}, M_{\Lambda^*}) &= \Gamma_{\Lambda}^* \left(\frac{p(M_{pK})}{p(M_{\Lambda^*})} \right)^{2L_{\Lambda^* \rightarrow pK}+1} \frac{M_{\Lambda^*}}{M_{pK}} F_{\Lambda^* \rightarrow pK}^2(p(M_{pK}), p(M_{\Lambda^*}))
 \end{aligned}$$

p, q Λ^*, K^- momentum in Λ_b, Λ^* restframe

F Blatt-Weißkopf form factors

$r_{\Lambda_b}, r_{\Lambda^*}$ Interaction radius of the Λ_b, Λ^*

$L_{\Lambda^* \rightarrow pK}$ orbital angular momentum difference between p and K^- in the $\Lambda^* \rightarrow pK^-$ decay

$L_{\Lambda_b \rightarrow \Lambda^* \mu\mu}$ orbital angular momentum difference between Λ^* and the dimuon system in the $\Lambda_b \rightarrow \Lambda^* \mu\mu$ decay

$M_{\Lambda^*}, \Gamma_{\Lambda^*}$ pole mass and width of Λ^*

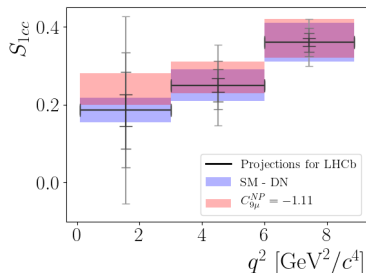
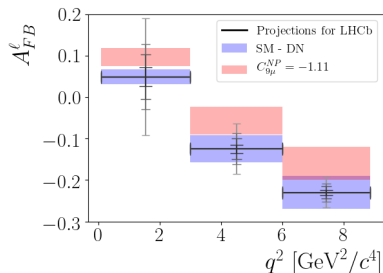
Dominating systematic uncertainties from $B_s^0 \rightarrow \phi\mu^+\mu^-$

Maximal systematic uncertainty with respect to statistical, called $\Delta u_{\text{sys}}/\Delta u_{\text{stat}}$ in $q^2 \in [1.1, 6] \text{ GeV}^2/c^4$ bin, from [JHEP 11 \(2021\) 043](#).

Source	$\Delta u_{\text{sys}}/\Delta u_{\text{stat}}$ [%]
Signal mass model	6.2
Angular acceptance order	0.3
Simulation correction	9.6
PID correction	1.1
Angular background model	5.6

Expected sensitivity in the future

Including only $\Lambda(1520)$ PDF, without $\Lambda_{1/2}$ contribution or background.
 Sensitivity with 9, 23, 50, 300 fb $^{-1}$ of data from [Eur. Phys. J. Plus 136, 614 \(2021\)](#).



Run 3 could help to separate between SM and preferred NP model.